An Exposed Tyrosine on the Surface of Trimethylamine Dehydrogenase Facilitates Electron Transfer to Electron Transferring Flavoprotein: Kinetics of Transfer in Wild-Type and Mutant Complexes†

Emma K. Wilson,‡ Liuxin Huang,§ Michael J. Sutcliffe,|| F. Scott Mathews,⊥ Russ Hille,§ and Nigel S. Scrutton*,‡

Departments of Biochemistry and Chemistry, University of Leicester, Adrian Building, University Road, Leicester LE1 7RH, U.K., Department of Medical Biochemistry, The Ohio State University, Columbus, Ohio 43210, and Department of Biochemistry and Molecular Biophysics, Washington University School of Medicine, St. Louis, Missouri 63110

Received May 22, 1996; Revised Manuscript Received September 11, 1996⊗

ABSTRACT: In wild-type trimethylamine dehydrogenase, tyrosine-442 is located at the center of a concave region on the surface of the enzyme that is proposed to form the docking site for the physiological redox acceptor, electron transferring flavoprotein. The intrinsic rate constant for electron transfer in the reoxidation of one-electron dithionite-reduced wild-type trimethylamine dehydrogenase (modified with phenylhydrazine) by electron transferring flavoprotein was investigated by stopped-flow spectroscopy. Analysis of the temperature dependence of the reaction rate by electron transfer theory yielded values for the reorganizational energy of 1.4 eV and the electronic coupling matrix element of 0.82 cm^{-1}. The role played by residue Tyr-442 in facilitating reduction of ETF by TMADH was investigated by isolating three mutant forms of the enzyme in which Tyr-442 was exchanged for a phenylalanine, leucine, or glycine residue. Rates of electron transfer from these mutants of TMADH to ETF were investigated by stopped-flow spectroscopy. At 25 °C, modest reductions in rate were observed for the Y442F (1.4-fold) and Y442L (2.2-fold) mutant complexes, but a substantial decrease in rate (30.5-fold) and an elevated dissociation constant for the complex were seen for the Y442G mutant enzyme. Inspection of the crystal structure of wild-type TMADH reveals that Tyr-442 is positioned along one side of a small cavity on the surface of the enzyme: Val 344, located at the bottom of this cavity, is the closest surface residue to the 4Fe-4S center of TMADH and is likely to be postioned on a major electron transfer pathway to ETF. The reduced electron transfer rates in the mutant complexes are probably brought about by decreases in electronic coupling between the electron transfer donor and acceptor within the complex, either directly or indirectly due to unfavorable change in the orientation of the two proteins with respect to one another.

The transient formation of weakly bound protein−protein complexes is a common feature of biological electron transfer. In many cases the components of these complexes are thought to associate initially in suboptimal configurations via nonspecific interactions and then undergo a diffusional search for the specific configuration commensurate with electron transfer—the so-called reduction-in-dimensionality principle (Northrup, 1996). The interactions involved in the formation of electron transfer complexes are poorly understood since the weaker protein−protein complexes are not generally accommodated in conventional structural techniques such as X-ray crystallography, although there are notable exceptions [e.g., Chen et al. (1994) and Merli et al., (1996)]. In addition, many physiological redox partners are membrane bound, thereby compounding the difficulties encountered with the structural determination of electron transfer complexes. Trimethylamine dehydrogenase (TMADH)[1] and electron transferring flavoprotein (ETF) from the methylotrophic bacterium *Methylophilus methylotrophus* (sp. W3A1) are soluble proteins that form a physiological electron transfer complex (Colby & Zatman, 1974; Steenkamp & Gallup, 1978) and represent a powerful system in which to examine the structure of a competent electron transfer complex.

Trimethylamine dehydrogenase (EC 1.5.99.7) is an iron−sulfur flavoprotein whose action is to convert trimethylamine to dimethylamine and formaldehyde (Steenkamp & Mallinson, 1976):

$$(CH_3)_3N + H_2O \rightleftharpoons (CH_3)_2NH + HCHO + 2e^- + 2H^+$$

Subsequent to reduction of TMADH by substrate, the electrons are passed individually in two sequential steps from the iron−sulfur center to the FAD of ETF, which cycles between the fully oxidized and semiquinone forms; full reduction to the dihydroquinone is only achieved by electrochemical means (Byron et al., 1989). TMADH is a homodimer, each subunit containing a 4Fe-4S center (Hill et al., 1977), a 6S-cysteinyl FMN (Steenkamp et al., 1978;

† This work was funded by grants from the Leverhulme Trust (N.S.S.), the Biotechnology and Biological Sciences Research Council (N.S.S.), the Royal Society (M.J.S. and N.S.S.), and the National Science Foundation (R.H.). E.K.W. was supported by a MRC Research Studentship.

* Corresponding author: telephone, +44 116 223 1337; Telefax, +44 116 252 3369; email, nss4@le.ac.uk.

‡ Department of Biochemistry, University of Leicester.

§ The Ohio State University.

|| Department of Chemistry, University of Leicester.

⊥ Washington University School of Medicine.

⊗ Abstract published in *Advance ACS Abstracts,* December 15, 1996.

[1] Abbreviations: TMADH, trimethylamine dehydrogenase; ETF, electron transferring flavoprotein; FAD, flavin adenine dinucleotide; FMN, flavin mononucleotide.

S0006-2960(96)01224-X CCC: $14.00

Kenney et al., 1978), and ADP. The function of the ADP is unknown, but it may represent the vestigial remains of an ancestral dinucleotide-binding site (Lim et al., 1988; Scrutton, 1994). TMADH forms binary and ternary complexes with ETF (Wilson et al., 1996), and the rates of electron transfer from reduced TMADH to oxidized ETF have been determined (Huang et al., 1995). Stopped-flow studies have shown that the overall rate-determining step with diethylmethylamine as substrate is product release (Rohlfs & Hille, 1994), although a recent study using trimethylamine has concluded that, at high concentrations of this substrate, the rate determining step may be associated with internal electron transfer from the 6S-cysteinyl FMN to the 4Fe-4S center (Falzon & Davidson, 1996). It is known that electron transfer from flavin to 4Fe-4S is not intrinsically rate-limiting in the absence of substrate (Rohlfs & Hille, 1991).

The genes encoding TMADH (Boyd et al., 1992) and ETF (Chen & Swenson, 1994) have been cloned, making the proteins amenable to genetic manipulation [e.g., see Scrutton et al. (1994), Packman et al. (1995), and Mewies et al. (1996)]. The crystal structure of TMADH has been solved at 2.4 Å resolution (Lim et al., 1986) and recently refined at 1.8 Å (S. A. White and F. S. Mathews, unpublished). A crystal structure for ETF is awaited (White et al., 1994). The crystal structure of TMADH reveals a large concave region (1200 $Å^2$) on its surface that is thought to be the interaction site for ETF (Wilson et al., 1995). A surface-exposed tyrosine residue (Tyr-442) is positioned at the center of this concave surface, close to the iron−sulfur center, where it is thought to mediate reduction of ETF by TMADH. The aromaticity at this position is conserved as a phenylalanine residue in the homologous position of the closely related enzyme dimethylamine dehydrogenase of *Hyphomicrobium X* (Yang et al., 1995), although no ETF from *Hyphomicrobium X* has yet been formally identified and the physiological partner to DMADH is unknown.

In this paper, we have examined the kinetics of electron transfer in wild-type and mutant TMADH·ETF electron transfer complexes, with the aim of identifying surface residues of TMADH that interact with ETF and potentiate electron transfer. We report the isolation and characterization of three mutant enzymes in which residue Tyr-442 is exchanged for a phenylalanine, leucine, or glycine residue. Stopped-flow kinetic studies of electron transfer from wild-type and mutant TMADH enzymes to ETF indicate that Tyr-442 facilitates electron transfer to ETF. The kinetic results demonstrate that Tyr-442 plays a role in both stabilizing the interaction between TMADH and ETF and accelerating electron transfer within the complex. The results confirm the previous postulate (Wilson et al., 1995) that the concave region on the surface of TMADH forms part of the interaction site for ETF.

EXPERIMENTAL PROCEDURES

Complex bacteriological media were from Difco Laboratories, and all media were prepared as described by Sambrook et al. (1989). Ultrapure agarose and cesium chloride were from Life Technologies Inc., ethidium bromide was from Bachem, and Timentin was from Beecham Research Laboratories. Sodium dithionite was purchased from Virginia Chemicals, phenylhydrazine from Eastman Kodak, and toluylene blue from Sigma and Aldrich library of rare chemicals. Ferricenium hexafluorophosphate was synthesized as described by Lehman et al. (1990). All other chemicals were of analytical grade wherever possible, and glass-distilled water was used throughout. Restriction enzymes *Eco*RI and *Hin*dIII were purchased from Pharmacia. Calf intestinal alkaline phosphatase was from Boehringer Mannheim. T4 DNA ligase and T4 polynucleotide kinase were from Amersham International.

Mutagenesis, Plasmid Construction, and DNA Sequencing. Bacteria were cultured in 2YT media supplemented where appropriate with Timentin. Plasmid DNA and bacteriophage RF DNA were prepared by cesium chloride density centrifugation, and general cloning methods were adopted from Sambrook et al. (1989). Site-directed mutagenesis was performed on a derivative of M13 containing the coding strand of the *tmd* gene as described previously (Scrutton et al., 1994). The mutagenic oligonucleotides 5′-CACGATAATCGCGGTGACCGCTCCACTCAC-3′ (Y442G), 5′-AATCGCGGTGGAAGCTCCACTCAC-3′ (Y422F), and 5′-CACGATAATCGCGGTGCAGGCTCCACTCAC-3′ (Y442L) were used to isolate bacteriophage constructs containing the desired mutations. Putative mutants were screened directly by dideoxynucleotide sequencing (Sanger et al., 1977) using the T7 system supplied by Pharmacia. Each mutant gene was resequenced in its entirety to ensure that spurious changes did not arise during the mutagenesis procedure. Each mutant gene was subcloned as an *Eco*RI/*Hin*dIII fragment into the expression construct pSV2tmdveg (Scrutton et al., 1994) where it replaced the analogous wild-type *Eco*RI/*Hin*dIII fragment.

Purification of Wild-Type and Mutant Proteins. Recombinant forms of TMADH were prepared from cultures of *Escherichia coli* strain TG1 transformed with the appropriate plasmid expression vector as described previously (Scrutton et al., 1994). TMADH was purified from *M. methylotrophus* (W3A1) as described by Steenkamp and Mallinson (1976) incorporating the modifications of Wilson et al. (1995). The flavin content of mutant enzymes was determined spectrophotometrically (Scrutton et al., 1994). The concentrations of mutant and wild-type TMADH enzymes were determined at 280 nm (ϵ_{280} = 201 610 M^{-1} cm^{-1}). TMADH was modified with phenylhydrazine as described by Nagy et al. (1979) and Kasprazak et al. (1983). ETF was purified from *M. methylotrophus* (W_3A_1) as previously described (Steenkamp & Gallup, 1978), except that the final gel filtration step was performed using Sephacryl 200-HR (Wilson et al., 1996). Complete oxidation of ETF was effected by treatment with potassium ferricyanide and desalted by chromatography using Sephadex G-25. The concentration of oxidized ETF was determined spectrophotometrically at 438 nm [ϵ_{438} = 11 300 M^{-1} cm^{-1} (Steenkamp & Gallup, 1978)].

Potentiometry. Potentiometric titrations of the FAD contained within ETF were conducted using the xanthine oxidase method developed by Massey (1990). ETF was contained in 50 mM potassium phosphate buffer, pH 7. Oxidized ETF (35 μM) was made anaerobic in a side-arm cuvette along with 250 μM xanthine, 2 μM methyl viologen, and 35 μM toluylene blue, total volume 1 mL; xanthine oxidase (8 μL of a 2.5 μM stock) was placed in the side arm of the apparatus. Following the achievement of anaerobosis by repeated evacuation and flushing with O_2-free argon, the UV−visible spectrum of the mix was recorded using a Hewlett Packard 8452a diode array spectrophotometer.

Reduction of the dye was initiated by tipping xanthine oxidase from the side arm into the mix. Spectra were recorded at 30 s intervals. The extent of reduction of ETF and the dye was determined from absorbance changes at 420 and 646 nm, respectively. The midpoint potential of ETF was determined from a plot of log $[ETF]_{ox}/[ETF]_{red}$ against log $[toluylene\ blue]_{ox}/[toluylene\ blue]_{red}$.

Steady-State and Stopped-Flow Kinetic Analyses. Steady-state kinetic parameters were determined at 25 °C in reaction mixtures containing 50 mM potassium phosphate, pH 7, and 100 μM trimethylamine. The concentration of TMADH was fixed and that of ETF varied. Reactions were initiated by the addition of trimethylamine. Reaction rates were calculated using a difference molar extinction coefficient between the oxidized and semiquinone forms of ETF (ϵ_{438} = 7830 M^{-1} cm^{-1}). Data were fitted to the Michaelis−Menten equation using the fitting program Kaleidograph (Abelbeck software, CA). Stopped-flow experiments were performed using a Kinetic Instruments Inc. stopped-flow apparatus equipped with an On-Line Instrument Systems (OLIS) Model 3920Z data collection system. Phenylhydrazine-treated TMADH was placed in a tonometer equipped with a ground glass joint (for the dithionite-titration syringe), a side-arm cuvette, and a three-way stopcock valve with a male Luer connector. The solution was made anaerobic by alternately evacuating and flushing with oxygen-free argon, and the iron−sulfur center of TMADH was reduced by titration with sodium dithionite. In stopped-flow experiments, the concentration of ETF was at least 5-fold greater than that of TMADH, thereby ensuring pseudo-first-order conditions. Kinetic transients were monitored as transmittance voltage, collected by a high-speed A/D converter, and converted into absorbance changes using OLIS software. Reactions were conducted in 50 mM potassium phosphate buffer, pH 7, and monitored at 370 nm (Huang et al., 1995). All data were best described by a single exponential (Figure 1), and rate constants were obtained by nonlinear least squares fitting to kinetic transients using the relationship:

$$\Delta A_t = \Delta A_o e^{-kt} \quad (1)$$

where ΔA_o represents the total absorbance change and ΔA_t the observed absorbance change at time t. Where saturation kinetic behavior was observed, plots of the observed rate constant against [ETF] were constructed and values for the limiting rate constant (k_{lim}) and the apparent dissociation constant K_d were calculated using the equation (Strickland et al., 1975):

$$k_{obs} = \frac{k_{lim}[ETF]}{[ETF] + K_d} \quad (2)$$

RESULTS

Kinetics of Transfer in Wild-Type and Mutant Complexes. Residue Tyr-442 is positioned at the center of a concave region on the surface of TMADH that is conjectured to form the ETF docking site (Figure 2; Wilson et al., 1995). It is the closest tyrosine to the iron−sulfur center and is in van der Waals contact with Val-344; the latter is adjacent in sequence to Cys-345, a ligand to one of the iron atoms. Since Tyr-442 protrudes into solution, forming no hydrogen bonds to other TMADH side chains, it was considered a likely candidate for interaction with the ETF. To probe the role of Tyr-442 in complex formation and subsequent electron transfer, we have constructed three mutant forms of TMADH in which the tyrosine residue was exchanged for a phenylalanine (as found in the related dimethylamine dehydrogenase), leucine, or glycine residue, and we have investigated

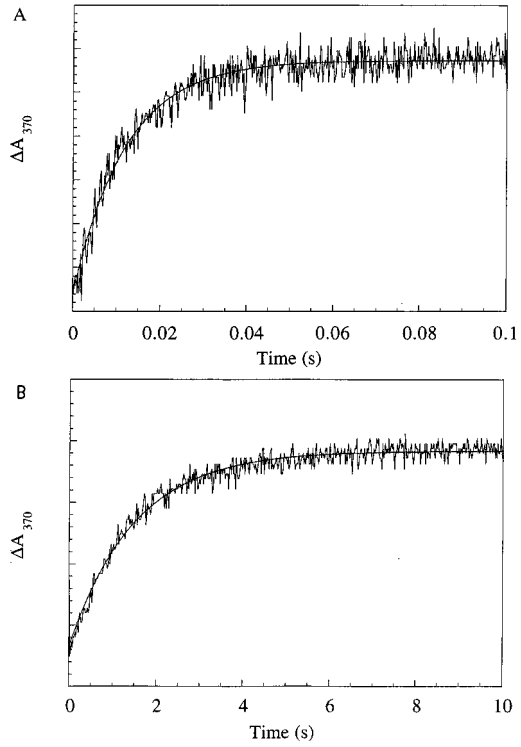

FIGURE 1: Kinetic transients observed for the wild-type (panel A) and Y442G mutant (panel B) complexes. Absorbance changes were recorded at 370 nm, and reaction components were contained in 50 mM potassium phosphate buffer, pH 7. The concentration of TMADH was 3.8 μM (wild type) and 3.8 μM (Y442G), and the concentrations of ETF were 36 μM (panel A) and 20 μM (panel B). The solid line represents the nonlinear least squares fit to the experimental data using eq 1.

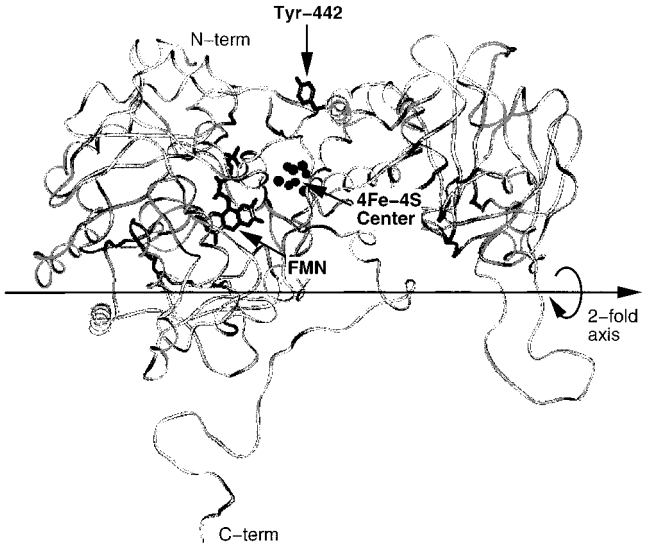

FIGURE 2: Molecular graphics of one subunit of TMADH showing the position of Tyr-442 at the center of the putative ETF docking site. All side chains are omitted with the exception of Tyr-442. The FMN and 4Fe-4S center are depicted. The representation is generated from the refined crystallographic coordinates of TMADH (F. S. Mathews and S. A. White, unpublished). Arrows indicate the approximate positions of the 2-fold axis of symmetry.

Table 1: Steady-State Kinetic Parameters for Wild-Type and Mutant Forms of TMADH[a]

enzyme	K_m(ETF) (μM)	k_{cat} (s^{-1})
wild type	17.5 ± 2	16.5 ± 0.8
Y442F	14.3 ± 3	10.3 ± 0.9
Y442L	19.6 ± 4	3.8 ± 0.3
Y442G	26.2 ± 5	0.25 ± 0.02

[a] The kinetic values are apparent and are measured at a trimethylamine concentration of 100 μM.

the detailed consequences of these alterations on the electron transfer kinetics to ETF.

In the steady state, plots of reaction rate against ETF concentration reveal that the reaction of wild-type and mutant forms of TMADH is described by simple Michaelis−Menten kinetics, (steady-state parameters are given in Table 1, with the observed Michaelis constants in the range 14.3−26.2 μM). Kinetic parameters are apparent and are measured using a trimethylamine concentration of 100 μM to avoid substrate-gated attenuation of the internal electron transfer in TMADH (Falzon & Davidson, 1996). The values of k_{cat} are found to decrease moderately for the Y442L mutant and substantially for the Y442G mutant, suggesting that removal of the aromatic side chain at residue 442 has compromised electron transfer from TMADH to ETF. Given that the rate-limiting step for the wild-type enzyme under the present experimental conditions is associated with product release in the reductive half-reaction, it seems likely from the steady-state data that the oxidative half-reaction, i.e., electron transfer to ETF, has become rate limiting in the Y442G mutant.

Electron transfer from TMADH to ETF can be monitored conveniently in the stopped-flow apparatus following modification of the C4a atom of the enzyme-bound flavin with phenylhydrazine (Nagy et al., 1979; Kasprzak et al., 1983). Modification renders the flavin redox inert, and the 4Fe-4S center can therefore be reduced selectively by titration with dithionite (Huang et al., 1995). This procedure limits reaction of enzyme to that with a single equivalent of ETF and simplifies the analysis of the oxidative half-reaction considerably; it has been used to follow the transfer of the electron from reduced wild-type TMADH to ETF (Huang et al., 1995). To extend this work, we have investigated the temperature dependence of the rate of electron transfer from the reduced 4Fe-4S center to ETF in the wild-type complex. Pseudo-first-order reactions were performed at 5, 15, 25, and 35 °C using a fixed concentration (3.8 μM) of phenylhydrazine-treated TMADH and various ETF concentrations ranging from 18 to 65 μM. The reaction at all temperatures was monophasic and exhibited saturation behavior with respect to the ETF concentration (Figure 3). The kinetically determined dissociation constant was similar at each temperature (range 15−25 μM), illustrating that increases in temperature over the selected range did not significantly affect complex assembly. The limiting values for electron transfer at each temperature are given in the legend of Figure 3. An Arrhenius plot of the k_{lim} values was linear and yielded an activation energy of 32.6 kJ mol^{-1}.

From the temperature perturbation data, it is possible to calculate the physical parameters governing the rate of electron transfer from the 4Fe-4S center to the FAD of ETF. The factors controlling the rate of electron transfer are

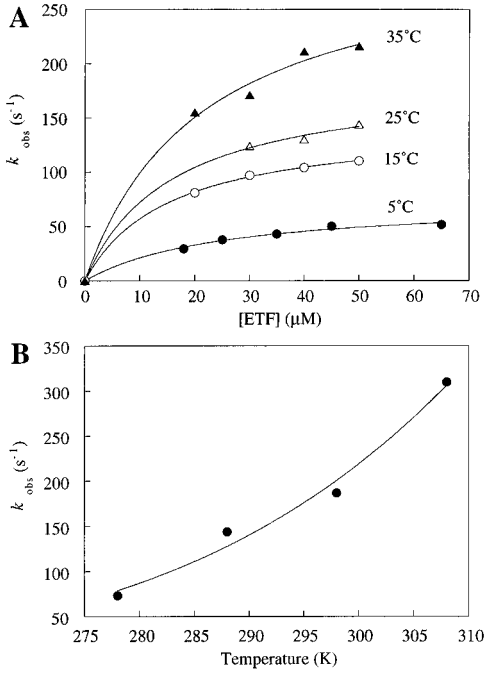

FIGURE 3: (Panel A) Plots of observed rate constant using stopped-flow against ETF concentration at 5, 15, 25, and 35 °C for the wild-type TMADH·ETF electron transfer complex. Data were fitted to eq 2. Limiting rate constants and kinetically determined dissociation constants are as follows: k_{lim} (s^{-1}) 73 ± 5, 143 ± 3, 187 ± 18, and 310 ± 34 at 5, 15, 25, and 35 °C, respectively; K_d (μM) 24.6 ± 4.5, 15.2 ± 1.1, 15.8 ± 5.4, and 21.2 ± 6 at 5, 15, 25, and 35 °C, respectively. (Panel B) Dependence of k_{lim} on temperature for the wild-type TMADH·ETF electron transfer complex. The solid line represents the fits of the data to eqs 3 and 4.

calculated from electron transfer theory (Marcus & Sutin, 1985), which relates the electron transfer rate (k_{ET}) as a function of free energy change ($\Delta G°$), temperature (T), the electronic coupling matrix element (H_{AB}), and the sum of the inner sphere (higher vibrational frequency of immediate ligands of the redox centers) and outer sphere (lower vibrational frequency of solvent and protein atoms) reorganizational energies (λ). The equation relating the nuclear and electronic factors to the rate of electron transfer is

$$k_{ET} = \frac{4\pi^2 H^2_{AB}}{h(4\pi\lambda RT)^{1/2}} e^{-(\Delta G°+\lambda)^2/4\lambda RT} \quad (3)$$

and consists of a classical component associated with nuclear motion and a quantum mechanical component (H^2_{AB}) associated with electron tunneling. R is the gas constant, h is Planck's constant, and T is the absolute temperature. Analysis of the temperature dependence of the electron transfer rate using eq 3 requires knowledge of $\Delta G°$ for the reaction, which is calculated as −3.76 kJ mol^{-1} from the known midpoint potential of the 4Fe-4S center (0.102 V; Barber et al., 1988) and the measured midpoint potential of ETF (0.141 V; Figure 4). Modification of TMADH with phenylhydrazine does not perturb the midpoint potential of the 4Fe-4S center (Barber et al., 1988). Analysis of the temperature dependence of electron transfer using eq 3 (Figure 3) yields values for the electronic coupling matrix element, H_{AB}, of 0.82 ± 0.58 cm^{-1} and the reorganizational energy, λ, of 136 ± 14 kJ mol^{-1} (1.4 eV). The value for λ (1.4 eV) calculated in this work is within a range of

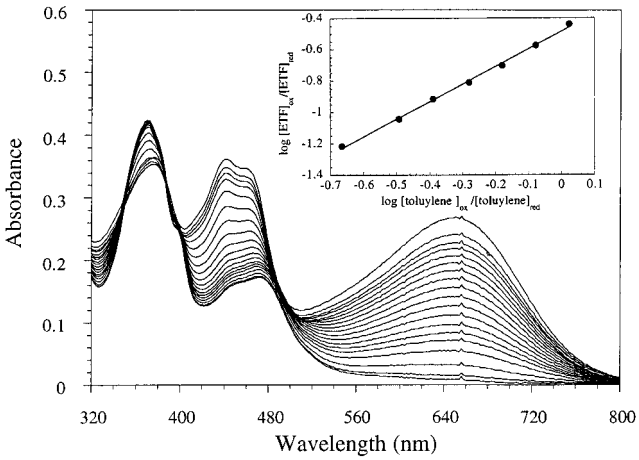

FIGURE 4: Midpoint potential determination of the FAD in ETF. Oxidized ETF (35 μM) contained in 50 mM potassium phosphate buffer, pH 7, was mixed with 35 μM toluylene blue, 2 μM methyl viologen, 250 μM xanthine, and 20 nM xanthine oxidase under anaerobic condtions. Scans were recorded every 30 s (not all data are shown). Inset: Plot of log $[ETF]_{ox}/[ETF]_{red}$ against log $[toluylene\ blue]_{ox}/[toluylene\ blue]_{red}$. Mid point redox potential is 0.141 V.

reorganizational energies measured for other biological electron transfer systems; e.g., $\lambda = 0.8-1.3$ eV has been reported for ruthenated proteins (Thieren et al., 1990), $\lambda =$ 0.7 eV for the bacterial photosynthetic reaction center (Moser et al., 1992), and $\lambda = 0.9$ eV for the cytochrome *c*−cytochrome b_5 complex (McLendon, 1988; Simmons et al., 1993). Larger values for λ have been measured for electron transfer between methanol dehydrogenase and cytochrome *c*-551i ($\lambda = 1.9$ eV; Harris & Davidson, 1993) and methylamine dehydrogenase and amicyanin ($\lambda = 2.3$ eV; Brooks & Davidson, 1994) and attributed to conformational changes and/or configurational realignment after complex formation for optimal electron transfer. The value of 1.4 eV calculated in this study is relatively large and may reflect such changes within the TMADH·ETF electron transfer complex. Since $-\Delta G^\circ << \lambda$ for TMADH → ETF electron transfer, the reaction is very much in the low driving force regime of the Marcus energy gap law, and consequently electron transfer rates are relatively slow. The value for H_{AB} (0.82 cm^{-1}) calculated in this work must be interpreted with caution since the intercept on fitting to eq 3 is poorly defined. For this reason, we wish not to place too much prominence on the value obtained for the electronic coupling matrix element.

A potential weakness with the analysis of the TMADH·ETF electron transfer kinetics using electron transfer theory is any variation that may arise in midpoint potential of the redox centers either as a consequence of complex formation or as a result of mutation of residue Tyr-442. However, since the reorganizational energy is substantially larger than the driving force for the reaction, any small alterations in ΔG° should not significantly affect the calculated parameters. For example, using the kinetic data measured for the wild-type complex, there is only a small change in the calculated reorganizational energy within the driving force range −13.4 to −0.39 kJ mol^{-1} ($\Delta E^{\circ\prime}$ range +139 to +4 mV). At the extremes of this range, the values for λ are within 18 kJ mol^{-1} (0.18 eV) of the value calculated for the TMADH·ETF complex and the values for H_{AB} are within 0.2 cm^{-1} of the calculated value for the wild-type complex.

Using electron transfer theory, the tunneling pathway distance, *r*, may be obtained from the equation:

$$k_{ET} = k_o e^{-\beta(r-r_o)} e^{-(\Delta G^\circ+\lambda)^2/4\lambda RT} \quad (4)$$

where k_o is the characteristic frequency of the nuclei and is assigned a value of 10^{13} s^{-1} (Marcus & Sutin, 1985; Rees & Farrelly, 1990) and r_o represents the van der Waals distance (3 Å). The electronic decay factor, β, is a coefficient that relates the decay of the electronic coupling matrix element as a function of distance, *r*. For homogeneous bridging material, the decay of the electronic coupling matrix element is given by Gamow's tunneling equation:

$$H_r^2 = H_o^2 e^{-\beta r} \quad (5)$$

where H_o is the tunneling matrix element at van der Waals separation. However, in proteins, the precise value of β changes throughout the tunneling pathway and depends on various factors, for example, whether the bridging structure is made up of covalent, hydrogen bond, or "through-space" connectivities (Beratan et al., 1991, 1992). Since most tunneling pathways in protein involve all three types of connectivity, the value of β has in some cases been averaged and approximated to 1.4 $Å^{-1}$ (Moser et al., 1992)—a value that is intermediate of that for covalently linked pathways ($\beta = 0.7$ $Å^{-1}$) and for pathways that pass through vacuum ($\beta = 2.8$ $Å^{-1}$). Using a β value of 1.4 $Å^{-1}$, a tunneling pathway distance of 11.3 ± 1 Å is obtained from eq 4 for the electron transfer event from TMADH to ETF. The calculated tunneling pathway distance is, however, very sensitive to the value of β selected (e.g., 19.6 Å for $\beta = 0.7$ $Å^{-1}$ and 7.2 Å for $\beta = 2.8$ $Å^{-1}$), and in some experimental systems predicted electron transfer rates using a value of 1.4 $Å^{-1}$ are at variance by as much as 2−3 orders of magnitude with the measured electron transfer rates [e.g., Wuttke et al. (1992a,b)]. Problems also arise in the definition of distance, i.e., the identification of the boundary between the donor and acceptor redox centers. With large redox centers such as the isoalloxazine of flavin and 4Fe-4S clusters this is a complicated issue, and measurements based on edge-to-edge distances (with $\beta = 0$ for intramolecular transmission within the redox center) may not be appropriate. Given our lack of knowledge of the value for β in TMADH and the strict meaning of pathway length, it is likely that the error in the tunneling pathway distance is large and it is in any case difficult to model this pathway distance into the crystal coordinates without a knowledge of the boundaries of the pathway. These complexities are in addition to those associated with calculating parameters from the intercept of Figure 3, as discussed above for the value of H_{AB}.

The role played by Tyr-442 in facilitating electron transfer to ETF has been investigated further by stopped-flow studies of electron transfer kinetics for mutant TMADH enzymes. As with native enzyme, each mutant was modified with phenylhydrazine prior to reduction with sodium dithionite, and studies of electron transfer as a function of [ETF] were conducted at 25 °C (Figure 5). The behavior of the Y442F and Y442L mutants was found to be similar to the behavior of the wild-type enzyme (k_{lim} 1.4- and 2.2-fold lower than wild type), but the limiting electron transfer rate for the Y442G mutant was found to be substantially lower than that for the wild type (6.1 *vs* 186 s^{-1}, representing a 30-fold

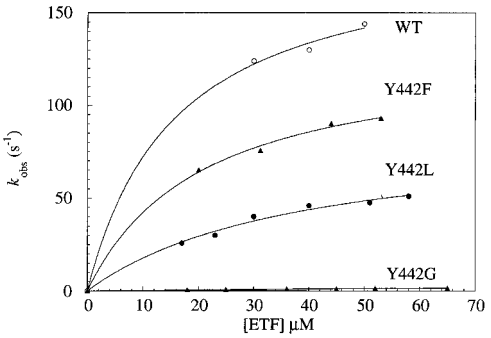

FIGURE 5: Plots of observed rate constant using stopped-flow against ETF concentration at 25 °C for the wild-type, Y442F, Y442L, and Y442G TMADH·ETF electron transfer complexes. Data were fitted to eq 2. Limiting rate constants and kinetically determined dissociation constants are as follows: k_{lim} (s^{-1}) 186 ± 18, 129 ± 6.8, 85.1 ± 8, and 6.1 ± 2 and K_d (μM) 15.8 ± 5.4, 20.6 ± 3, 37.8 ± 7.7, and 179 ± 70 for the wild-type, Y442F, Y442L, and Y442G complexes, respectively.

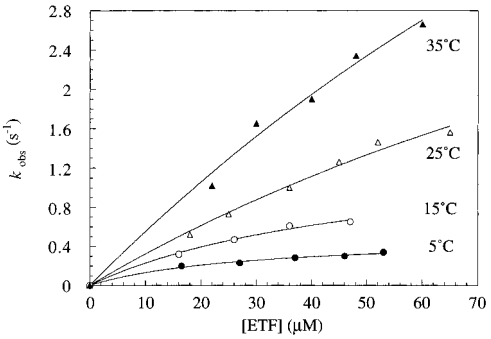

FIGURE 6: Plots of observed rate constant using stopped-flow against ETF concentration at 5, 15, 25, and 35 °C for the Y442G TMADH·ETF electron transfer complex. Data were fitted to eq 2. Limiting rate constants and kinetically determined dissociation constants are as follows: k_{lim} (s^{-1}) 0.5 ± 0.05, 1.3 ± 0.24, 6.1 ± 2, and 12.2 ± 6 at 5, 15, 25, and 35 °C, respectively; K_d (μM) 28.2 ± 7, 50.8 ± 14, 179 ± 70, and 211 ± 126 at 5, 15, 25, and 35 °C, respectively.

reduction in k_{lim}). In addition, mutation of Tyr-442 to glycine resulted in a 10-fold increase in K_d (179 μM, as compared to 15.8 μM for the wild-type enzyme), giving an overall effect on k_{lim}/K_d (which corresponds to the second-order rate constant for electron transfer in the low [ETF] regime) of 300. The kinetically determined dissociation constant for the Y442G mutant TMADH was also found to be about 1 order of magnitude higher than the same parameter for the wild-type, Y442F, and Y442L mutant enzymes.

The substantial reduction in electron transfer rate for the Y442G mutant enzyme and the higher dissociation constant observed at 25 °C prompted us to conduct a temperature perturbation analysis of electron transfer for this enzyme. As with the wild-type complex, stopped-flow experiments were conducted at 5, 15, 25, and 35 °C. Over this temperature range, k_{lim} rose from 0.5 to 12.2 s^{-1}, but perhaps more importantly the dissociation constant for the complex was raised by 1 order of magnitude (Figure 6). At 5 °C, the dissociation constant for the Y442G·ETF complex is similar to the dissociation constant for the wild-type TMADH·ETF complex at all temperatures studied and the Y442F·ETF and Y442L·ETF complexes studied at 25 °C. The effect of mutating Tyr-442 to a glycine residue is, therefore, to impair complex assembly ($\Delta G_{Y442G} - \Delta G_{WT} = 5.88$ kJ mol^{-1} at 35 °C) in addition to compromising the electron transfer rate to ETF. We were unable to calculate values for r, H_{AB}, and λ for the Y442G mutant enzyme because, unlike for the wild-type complex, the dissociation constant for the Y442G·ETF complex was found to be extremely temperature dependent, with the result that the reorganizational energy would not be constant over the temperature range studied. A change in the structure of the productive electron transfer complex as a function of temperature may also alter the tunneling pathway distance. For these reasons, it was judged inappropriate to analyze the data in the manner described for the wild-type complex.

Geometrical Considerations of the Electron Transfer Complex and the Potential Role of Tyr-442. The observations described above illustrate that Tyr-442 is involved in facilitating electron transfer from TMADH to ETF. However, the precise role of this residue remains to be established. The aromatic ring of Tyr-442 is situated along the side of a surface cavity in TMADH (Figures 2 and 7). Val-344 is located at the base of this cavity, adjacent in sequence to one of the cysteinyl ligands (Cys-345) of the 4Fe-4S cluster, and this residue could provide a direct electron transfer pathway from the 4Fe-4S center to ETF. Using the Pathways algorithm (Beratan & Onuchic, 1996), an alternative potential electron transfer pathway has also been identified using Tyr-442 as the "conduit". The pathway passes through the cysteinyl ligand of Cys-345, along the protein backbone to its carbonyl oxygen, through space to a carboxyl oxygen of Glu-439, and finally through space to Tyr-442. A recent determination of the crystal structures of human and *Paracoccus denitrificans* ETF molecules [about 30% amino acid sequence identity with the *M. methylotrophus* ETF in both subunits (Chen & Swenson, 1994)] indicates that the C7 methyl of the flavin is solvent exposed with the FAD isoalloxazine located close to a cleft between the two subunits of the protein (Roberts et al., 1996). Assuming that *M. methylotrophus* ETF is of similar structure, the C7 methyl would be likewise solvent exposed and may be located close to the surface cavity identified on the surface of TMADH during complex formation. Recent solution studies in the analytical ultracentrifuge (Cölfen et al., 1996) indicate that the ETF of *M. methylotrophus* is a dynamic molecule that reversibly dissociates (K_d 1.5 μM) into two subunits at low concentrations. The observed flexibility of ETF may allow the FAD to adopt different conformations during complex assembly than would be surmised from the crystal structure of ETF alone, especially since the FAD is bound at the subunit interface of the human and *P. denitrificans* ETF molecules.

DISCUSSION

In recent years, the individual steps in the reaction catalyzed by trimethylamine dehydrogenase have been investigated in detail. The reductive half-reaction with the slow substrate diethylmethylamine is clearly resolved into three catalytic steps (Rohlfs & Hille., 1994), *viz.*, a fast phase that is dependent on substrate concentration and represents reduction of the flavin, an intermediate phase that is proposed to involve the breakdown of a covalent substrate−flavin intermediate, and a slow phase associated with product release (the rate-determining step at low substrate concentrations). Internal electron transfer from the flavin to the 4Fe-4S center has also been evaluated. In the absence of substrate, pH-jump stopped-flow experiments have indicated

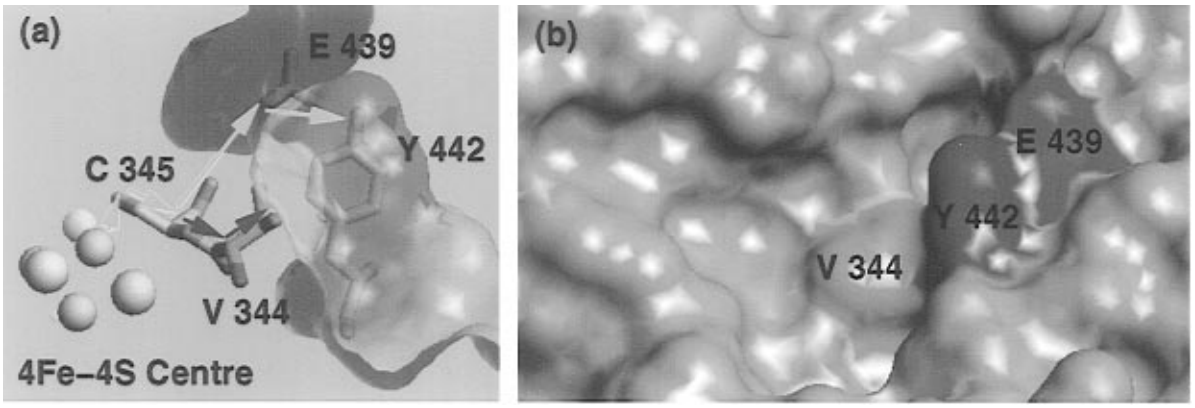

FIGURE 7: Structure of the cavity on the surface of TMADH and potential electron transfer pathways to the surface of the enzyme. (a) Side view, showing two possible electron transfer pathways from the 4Fe-4S center via Cys-345 either to Glu-439 and then Tyr-442 (yellow arrows) or to Val-344 (red arrows). (b) View from above, showing the molecular surface, illustrating the surface cavity and the positions of Tyr-442 (purple), Val-344 (blue), and Glu-439 (green).

that this step is not intrinsically rate limiting (Rohlfs & Hille, 1991), but the presence of substrate influences the rate of electron transfer from the reduced flavin to the 4Fe-4S center (Huang et al., 1995; Falzon & Davidson, 1996), perhaps reflecting coupling to protonation/deprotonation events (Rohlfs et al., 1995) and/or conformational gating. More recently, attention has focused on the oxidative half-reaction and more specifically on electron transfer from the 4Fe-4S center of wild-type TMADH to ETF (Huang et al., 1995), a step that is not rate limiting in the overall reaction. This work has demonstrated that reducing equivalents are transferred from TMADH to ETF solely through the 4Fe-4S center with an intrinsic rate constant of 172 s^{-1} and dissociation constant of 10 μM. Reoxidation of substrate-reduced wild-type TMADH with the artificial redox acceptor ferricenium hexafluorophosphate has also been investigated (Wilson et al., 1995) and the kinetic behavior analyzed using electron transfer theory. Biphasic kinetic behavior for the reduction of ferricenium ions is observed and attributed to two independent sequential electron transfers from the 4Fe-4S center of TMADH. More recent work, however, suggests that the simple kinetic model developed in this work is overly simplistic and that the complexities of the kinetics may be caused by the existence of multiple binding sites for ferricenium ions on TMADH (E. K. Wilson and N. S. Scrutton, unpublished). For this reason, in this work we have reinvestigated the oxidative half-reaction using the physiological redox acceptor, ETF. We have also isolated three mutant TMADH enzymes altered in the identity of the residue at position 442 to investigate the role of Tyr-442 in the wild-type enzyme in facilitating electron transfer to ETF.

A temperature perturbation analysis of electron transfer in wild-type TMADH·ETF complexes has permitted calculation of values for H_{AB}, λ, and the tunneling pathway distance, r, although due to the nature of the equations used in data fitting and as described above, there can be confidence only in the calculated value for λ. The values for the remaining two parameters (H_{AB} and r) are subject to wide variation depending on either the nature of the equations used to fit the data or the chosen value for the electronic decay factor, β, which is itself subject to variation depending on the properties of the bridging protein structure.

The measured electron transfer kinetics of the mutant TMADH enzymes studied here serve to illustrate that Tyr-442 facilitates electron transfer to ETF. Mutation of this residue to glycine severely compromises the electron transfer rate to the flavin of ETF, increasing the K_d by a factor of 10 and decreasing the limiting rate constant for electron transfer within the complex by 30-fold. The question that follows from this work pertains to the actual role of Tyr-442 in the TMADH·ETF complex: the residue may direct protein−protein interactions between ETF and TMADH (the surface cavity of TMADH being filled by residues contributed by ETF during electron transfer complex formation) and/or may also play a more direct role in electronic coupling between the electron transfer donor and acceptor sites. Examination of the TMADH structure identifies Val-344 as providing a possible, direct, electron transfer route from the 4Fe-4S center to the FAD. Val-344 lies at the bottom of the pocket formed partially by Tyr-442 (Figure 7) and is immediately N-terminal to Cys-345, a cysteinyl ligand of the 4Fe-4S center. With respect to Tyr-442, the Pathways algorithm identifies a possible electron transfer pathway that passes through Cys-345, Glu-439, and Tyr-442. Tyr-442 is located on a helix, and mutation to glycine may perturb the local structure in this region of the protein in such a way that ETF and TMADH are misaligned to some degree in the Y442G mutant complex. One might expect the mutations Y442F and Y442L should not affect structure in this region of the protein to the same extent as the Y442G mutation. It is therefore reassuring that the electron transfer rates in these two mutant proteins were found to be only modestly affected as a result of mutation. The identification of any structural readjustments in the mutant enzymes, however, must await a crystallographic solution for each of the mutant proteins; this work is currently in progress.

In the present work, we have established that Tyr-442 plays a significant role in facilitating electron transfer from TMADH to ETF. The precise role of this residue remains to be established, but our results suggest that it may play a role in the binding of ETF at the surface of TMADH. The location of Tyr-442, and by implication the binding site for ETF, at the center of the concave region on the surface of TMADH is entirely consistent with our previous ultracentrifugal analysis of complex assembly. Evidence for ternary complex (TMADH·2ETF) formation as well as binary complex formation (TMADH·ETF) has been reported from ultracentrifugal work (Wilson et al., 1996), and therefore binding of one molecule of ETF to TMADH must not sterically impair the binding of a second ETF molecule.

Inspection of the crystal structure of TMADH reveals that the location of the concave putative ETF-interaction regions on the surface of the dimer is compatible with ternary complex formation, in that the region on the surface of TMADH monomer implicated here in binding ETF is not near the subunit interface region of TMADH. Given that the two subunits of TMADH are thought to operate independently of one another, it is expected that there will be no kinetic manifestation of this ternary complex. The work described in this paper now provides a focus for future studies of the interaction between TMADH and ETF. The pertinent questions that remain are (i) what is the extent of the interaction site for ETF on the surface of TMADH and (ii) what are the forces that guide the formation of the optimally configured electron transfer complex? These questions are presently being addressed using structural, kinetic, and mutagenesis methods.

REFERENCES

Barber, M. J., Pollock, V., & Spence, J. T. (1988) *Biochem. J. 256*, 657−659.

Beratan, D. N., & Onuchic, J. N. (1996) in *Protein Electron Transfer* (Bendall, D. S., Ed.) pp 23−42, Bios Scientific Publishers, Oxford.

Beratan, D. N., Betts, J. V., & Huddleston, R. K. (1991) *Science 252*, 1285−1288.

Beratan, D. N., Betts, J. V., & Onuchic, J. N. (1992) *J. Phys. Chem. 96*, 2852−2855.

Boyd, G., Mathews, F. S., Packman, L. C., & Scrutton, N. S. (1992) *FEBS Lett. 308*, 271−276.

Brooks, H. B., & Davidson, V. L. (1994) *Biochemistry 33*, 5696−5701.

Byron, C. M., Stankovich, M. T., Husain, M., & Davidson, V. L. (1989) *Biochemistry 28*, 8582-8587.

Chen, D. W., & Swenson, R. P. (1994) *J. Biol. Chem. 269*, 32120−32128.

Chen, L., Durley, R. C. E., Mathews, F. S., & Davidson, V. L. (1994) *Science 264*, 86−90.

Colby, J., & Zatman, L. J. (1974) *Biochem. J. 143*, 555−567.

Cölfen, H. C., Harding, S. E., Wilson, E. K., Scrutton, N. S., & Winzor, D. J. (1996) *Eur. Biophys. J.* (in press).

Falzon, L., & Davidson, V. L. (1996) *Biochemistry 35*, 2445−2452.

Harris, T. K., & Davidson, V. L. (1993) *Biochemistry 32*, 14145−14150.

Hill, C. L., Steenkamp, D. J., Holm, R. H., & Singer, T. P. (1977) *Proc. Natl. Acad. Sci. U.S.A. 74*, 547−551.

Huang, L., Rohlfs, R. J., & Hille, R. (1995) *J. Biol. Chem. 270*, 23958−23965.

Kasprazak, A. A., Papas, E. J., Steenkamp, D. J. (1983) *Biochem. J. 211*, 535−541.

Kenney, W. C., McIntire, W. S., Steenkamp, D. J., & Benisek, W. F. (1978) *FEBS Lett. 85*, 137−139.

Lehman, T. C., Hale, D. E., Bhala, A., & Thorpe, C. (1990) *Anal. Biochem. 186*, 280−284.

Lim, L. W., Shamala, N., Mathews, F. S., Steenkamp, D. J., Hamlin, R., & Xuong, N. H. (1986) *J. Biol. Chem. 261*, 15140−15146.

Lim, L. W., Mathews, F. S., & Steenkamp, D. J. (1988) *J. Biol. Chem. 263*, 3075−3078.

Marcus, R. A., & Sutin, N. (1985) *Biochim. Biophys. Acta 811*, 265−322.

Massey, V. (1990) in *Flavins and Flavoproteins* (Curti, B., Ronchi, S., & Zanetti, G., Eds.) pp 59−66, Walter de Gruyter, Berlin.

McLendon, G. (1988) *Acc. Chem. Res. 21*, 160−167.

Merli, A., Brodersen, D. E., Morini, B., Chen, Z.-W., Durley, R. C. E., Mathews, F. S., Davidson, V. L., & Rossi, G. L. (1996) *J. Biol. Chem. 271*, 9177−9180.

Mewies, M., Packman, L. C., Mathews, F. S., & Scrutton, N. S. (1996) *Biochem. J. 317*, 267−272.

Moser, C. C., Keske, J. M., Warncke, K., Farid, R. S., & Dutton, P. L. (1992) *Nature 355*, 796−802.

Nagy, J., Kenney, W. C., & Singer, T. P. (1979) *J. Biol. Chem. 254*, 2684−2688.

Northtrup, S. H. (1996) in *Protein Electron Transfer* (Bendall, D. S., Ed.) pp 69−98, Bios Scientific Publishers, Oxford.

Packman, L. C., Mewies, M., & Scrutton, N. S. (1995) *J. Biol. Chem. 270*, 13186−13195.

Rees, D. C., & Farrelly, D. (1990) in *The Enzymes*, Vol. 19, pp 37−96, Academic Press, Inc., New York.

Roberts, D. L., Frerman, F. E., & Kim, J.-J. (1996) in *Flavins and Flavoproteins* (Stevenson, K. J., Massey, V., & Williams, C. H., Jr., Eds.) University of Calgary Press, Calgary (in press).

Rohlfs, R. J., & Hille, R. (1991) *J. Biol. Chem. 266*, 15244−15252.

Rohlfs, R. J., & Hille, R. (1994) *J. Biol. Chem. 269*, 30869−30879.

Sambrook, J., Fritsch, E. F., & Maniatis, T. (1989) in *Molecular cloning: a laboratory manual*, 2nd ed., Cold Spring Harbor Laboratory, Cold Spring Harbor, NY.

Sanger, F., Nicklen, S., & Coulson, A. R. (1977) *Proc. Natl. Acad. Sci. U.S.A. 74*, 5463−5467.

Scrutton, N. S. (1994) *BioEssays 16*, 115−122.

Scrutton, N. S., Packman, L. C., Mathews, F. S., Rohlfs, R. J., & Hille, R. (1994) *J. Biol. Chem. 269*, 13942−12950.

Simmons, J., McLendon, G., & Qiao, T. (1993) *J. Am. Chem. Soc. 115*, 4889−4890.

Steenkamp, D. J., & Mallinson, J. (1976) *Biochim. Biophys. Acta 429*, 705−719.

Steenkamp, D. J., & Gallup, M. (1978) *J. Biol. Chem. 253*, 4086−4089.

Steenkamp, D. J., McIntire, W. S., & Kenney, W. C. (1978) *J. Biol. Chem. 253*, 2818−2828.

Strickland, S., Palmer, G., & Massey, V. (1975) *J. Biol. Chem. 250*, 4048−4052.

Thieren, M. J., Selman, M. A., Gray, H. B., Chang, I. J., & Winkler, J. R. (1990) *J. Am. Chem. Soc. 112*, 2420−2422.

White, S. A., Mathews, F. S., Rohlfs, R. J., & Hille, R. (1994) *J. Mol. Biol. 240*, 265−266.

Wilson, E. K., Mathews, F. S., Packman, L. C., & Scrutton, N. S. (1995) *Biochemistry 34*, 2584−2591.

Wilson, E. K., Scrutton, N. S., Cölfen, H., Harding, S. E., & Winzor, D. J. (1996) *Eur. J. Biochem.* (in press).

Wuttke, D. S., Bjerrum, M. J., Winkler, J. R., & Gray, H. B. (1992a) *Science 256*, 1007−1009.

Wuttke, D. S., Bjerrum, M. J., Chang, I.-J., Winkler, J. R., & Gray, H. B. (1992b) *Biochim. Biophys. Acta 1101*, 168−170.

Yang, C.-C., Packman, L. C., & Scrutton, N. S. (1995) *Eur. J. Biochem. 232*, 264−271.

BI961224Q